

Entanglement and inversion symmetry in topological insulators

Ari M. Turner, Yi Zhang, and Ashvin Vishwanath

Department of Physics, University of California, Berkeley, California 94720, USA

(Received 10 October 2010; published 13 December 2010)

Topological band insulators are usually characterized by symmetry-protected surface modes or quantized linear-response functions (like Hall conductance). Here we present a way to characterize them based on certain bulk properties of just the ground-state wave function, specifically, the properties of its entanglement spectrum. We prove that whenever protected surface states exist, a corresponding protected “mode” exists in the entanglement spectrum as well. Besides this, the entanglement spectrum sometimes succeeds better at indicating topological phases than surface states. We discuss specifically the example of insulators with inversion symmetry which is found to act as an antiunitary symmetry on the entanglement spectrum. A Kramers degeneracy can then arise even when time-reversal symmetry is absent. This degeneracy persists for interacting systems. The entanglement spectrum is therefore a promising tool to characterize topological band insulators and superconductors beyond the free-particle approximation.

DOI: [10.1103/PhysRevB.82.241102](https://doi.org/10.1103/PhysRevB.82.241102)

PACS number(s): 73.20.At, 03.67.–a, 03.65.Vf

According to the Landau Paradigm, distinct phases of systems can be classified according to their pattern of symmetry breaking. A phase can therefore be identified by the appearance of a nonzero expectation value for the spin (or another variable breaking the symmetry). It has been known for a while now that this is not the only way to distinguish between phases. For example, a topological distinction can also lead to a sharp definition of a phase. Even for noninteracting fermions, in an insulating phase, it is possible to distinguish between different topological classes. There is a trivial type of insulator, corresponding to the standard picture of bringing isolated atoms with filled sets of orbitals together, and there are nontrivial phases known as topological insulators¹ that can occur when electrons occupy bonding orbitals shared between atoms. These include the quantum Hall Chern insulators and the more recently discovered spin-orbit topological insulators.

Our goal is to describe a *bulk* property, like the order parameters of Landau, that can be used to distinguish between trivial and nontrivial topological insulators. Moreover, we expect this information to be present in the ground-state wave function since it is not possible to pass from a trivial to a nontrivial insulator without a phase transition in the bulk. We will seek the signature in the entanglement spectrum of the insulator when cut in two. Any insulator except for perfectly isolated atoms has nonzero entanglement. But for the topological insulator, the entanglement cannot be eliminated continuously. The entanglement *spectrum* (introduced by Ref. 2) has a qualitative property that guarantees a nonzero entanglement entropy, as shown below.

The most concrete property of most topological insulators is that its surface is metallic although the bulk is insulating. Our first goal will be to deduce from this the robustness of the entanglement: if physical surface modes exist throughout a certain phase, then “entanglement modes” on an imaginary cutting surface exist as well (also shown independently by Ref. 3). This result applies to quantum Hall states,⁴ spin quantum Hall states, and topological insulators,⁵ which have been treated earlier on a case-by-case basis. It also can be generalized to describe entanglement of topological superconductors⁶ (when pairing is allowed).

Our main result is that the entanglement spectrum some-

times reveals *more* than the surface spectrum does. Spin-orbit topological insulators require the presence of a symmetry, time reversal, for their definition, but one can consider instead insulators that are symmetric under inversion symmetry in a point. The inversion symmetry turns out to protect modes in the entanglement spectrum (even when surface modes are gapped) because inversion symmetry acts in a special way on the entanglement spectrum. On the single-body modes, inversion acts like a particle-hole symmetry; on many-body entanglement states it is antiunitary.

Given the ground-state wave function, and a partition of the system into a left and right half, one can perform a Schmidt decomposition

$$|G\rangle = \sum_{\alpha} \frac{1}{\sqrt{Z}} e^{-E_{\alpha}^e/2} |\alpha L\rangle |\alpha R\rangle. \quad (1)$$

Measuring the left half of the system shows it to be in state $|\alpha L\rangle$ with probability $e^{-E_{\alpha}^e}/Z$. The quantities E_{α}^e form the entanglement spectrum; they are the eigenvalues of the “entanglement Hamiltonian” H^e and are somewhat like “energies” since they characterize how unlikely a given fluctuation is to occur. (We use the superscript “e” when describing the entanglement.)

For a noninteracting wave function, according to Refs. 7 and 8, these many-body entanglement energies can be written as sums of single-particle entanglement energies

$$E_{\alpha}^e = \sum_{i, \mathbf{k}_{\perp}} n_i^{\alpha}(\mathbf{k}_{\perp}) \epsilon_i^e(\mathbf{k}_{\perp}). \quad (2)$$

Here, i indexes the bands, and $n_{i\mathbf{k}_{\perp}}^{\alpha} = 0, 1$ is the occupation number of mode i for the many-body state α . Because the cutting surface is translationally symmetric, one can classify the modes by their momentum² \mathbf{k}_{\perp} parallel to the cut, allowing one to consider band-structure graphs, rather than a continuum of overlapping energy levels. The dispersions $\epsilon_i^e(\mathbf{k}_{\perp})$ are related to the eigenenergies $p_i(\mathbf{k}_{\perp})$ of a Hamiltonian H_{flat} that is in the same topological class as the physical Hamiltonian (see below). Therefore, if the phase of the system has protected surface modes, the physical system does too.

Review of entanglement of noninteracting fermions. The spectrum can be determined by decomposing the insulator

into independent one-electron modes,⁸ each of which contributes a term to the entanglement energy, Eq. (2). Consider the state of a single electron $c^\dagger|Vac\rangle$, where c^\dagger creates $F(\mathbf{r})$. This mode may be split into its parts on the left and right side of the surface, $F(\mathbf{r}) = \sqrt{p}f_L(\mathbf{r}) + \sqrt{1-p}f_R(\mathbf{r})$. (The factors of $\sqrt{p}, \sqrt{1-p}$ are normalizations.) Therefore $c^\dagger|Vac\rangle = \sqrt{p}(l^\dagger|VacL\rangle|VacR\rangle) + \sqrt{1-p}(|VacL\rangle r^\dagger|VacR\rangle)$, (where l^\dagger and r^\dagger create the f_L and f_R states). This gives the Schmidt decomposition of the mode: either there is an electron on the left and a hole on the right or vice versa. The entanglement Hamiltonian which gives the right relative probabilities for the two states on the left is $H^e = \epsilon l^\dagger l$, where $\frac{p}{1-p} = e^{-\epsilon}$.

For many electrons occupying many modes $F_{i\mathbf{k}_\perp}$, the same method can be applied one mode at a time provided they are independent. This independence condition, formulated by Ref. 7, requires that the modes appearing in the decomposition

$$F_{i\mathbf{k}_\perp} = [\sqrt{p_i(\mathbf{k}_\perp)}f_{Li\mathbf{k}_\perp}(x) + \sqrt{1-p_i(\mathbf{k}_\perp)}f_{Ri\mathbf{k}_\perp}(x)]e^{i\mathbf{k}_\perp \cdot \mathbf{r}_\perp}, \quad (3)$$

namely, $f_{Li\mathbf{k}_\perp}$ and $f_{Ri\mathbf{k}_\perp}$, each form orthonormal sets. This orthonormality condition is equivalent to an eigenvalue problem for f_L . They must satisfy $\sum_{x<0}^{r=(x,y,z)} C(\mathbf{r}, \mathbf{r}') f_{Li\mathbf{k}_\perp}(\mathbf{r}) = p_i(\mathbf{k}_\perp) f_{Li\mathbf{k}_\perp}(\mathbf{r}')$, where $C(\mathbf{r}, \mathbf{r}')$ is the correlation function of the ground state. (Spin and orbital indices should be added along with the spatial coordinates.) The entanglement Hamiltonian is then $\sum_{i\mathbf{k}_\perp} \epsilon_i^e(\mathbf{k}_\perp) l_{i\mathbf{k}_\perp}^\dagger l_{i\mathbf{k}_\perp}$, where

$$\frac{1}{2} \tanh \frac{\epsilon_i^e(\mathbf{k}_\perp)}{2} = \frac{1}{2} - p_i(\mathbf{k}_\perp). \quad (4)$$

This gives an efficient way to compute the entanglement spectrum: calculate $C(\mathbf{r}, \mathbf{r}')$, restrict to the left half of the system and diagonalize.

Topological protection of entanglement modes. This description of the entanglement modes has an intuitive interpretation: the modes p_i are the surface modes of an insulator in $x < 0$ with the following hopping matrix:

$$H_{flat\mathbf{r}\mathbf{r}'} = \frac{1}{2} \delta_{\mathbf{r}\mathbf{r}'} - C(\mathbf{r}, \mathbf{r}'). \quad (5)$$

Since the correlation function decays exponentially with distance, this Hamiltonian could conceivably describe a physical system with hopping mostly to nearby neighbors.

Now this Hamiltonian has a simple relationship to the actual Hamiltonian; if the latter's plane-wave modes are $H = \sum_\gamma \epsilon_\gamma(\mathbf{k}) a_{\mathbf{k}\gamma}^\dagger a_{\mathbf{k}\gamma}$, where $a_{\mathbf{k}\gamma}$ refers to the Bloch states, then H_{flat} has these same eigenstates but associated with different energy dispersions. The bands are flat and degenerate for all occupied bands and all unoccupied bands, i.e., $H_{flat} = \sum_\gamma \epsilon_{F\gamma} a_{\mathbf{k}\gamma}^\dagger a_{\mathbf{k}\gamma}$ with

$$\epsilon_{F\gamma}(\mathbf{k}) = -\frac{1}{2} \text{ if } \gamma \text{ is an occupied band,} \quad (6)$$

$$\epsilon_{F\gamma}(\mathbf{k}) = +\frac{1}{2} \text{ if } \gamma \text{ is an unoccupied band.} \quad (7)$$

The proof of the topological protection of entanglement modes can now be completed: H_{flat} is in the same phase as H

since the bands can be flattened without ever crossing the Fermi level. Therefore, if H is in a phase with *protected* surface modes, then H_{flat} has surface modes too, and they must cross the bulk gap between $+\frac{1}{2}$ and $-\frac{1}{2}$. Since these modes' dispersion is $\frac{1}{2} \tanh \frac{\epsilon_i^e(\mathbf{k}_\perp)}{2}$, there are zero-energy entanglement modes. In particular, there are many Schmidt states with equal weights, corresponding to zero "energy," and thus continuously changing the system cannot bring the entanglement entropy to zero, as it is in a crystal of uncommunicating atoms.

Topological Protection in three-dimensional time-reversal symmetric insulators. We will now illustrate this result for topological insulators. Some classes of topological phases require a symmetry for their protection; for topological insulators, this is time reversal. Topological insulators have an odd number of metallic Dirac nodes on their surfaces, located at the four surface TRIMs κ_\perp (the "time-reversal invariant momenta" modulo the reciprocal lattice). In Figs. 1(a) and 1(b) are depicted the surface modes and entanglement modes of a strong topological insulator, given by a spin-orbit model on a diamond lattice⁹

$$H = \sum_{ij} t_{ij} c_{i\sigma}^\dagger c_{j\sigma} + 8i\lambda_{SO} \sum_{\langle\langle ik \rangle\rangle} c_{i\sigma}^\dagger (\mathbf{d}_{ik}^1 \times \mathbf{d}_{ik}^2) \cdot \boldsymbol{\sigma}_{\sigma\sigma'} c_{k\sigma'}, \quad (8)$$

where the first term contains the four nearest-neighbor hopping elements which are taken as t for three of the bonds, and $t + \delta t$ for the fourth bond oriented along the $(-1, 1, -1)$ direction; we will also add a second-neighbor hopping t_2 which is the same for all directions. The spin-orbit interaction appears in the second term, inducing hopping between second-neighbor sites. In this term, $\mathbf{d}_{ik}^1, \mathbf{d}_{ik}^2$ are the two nearest-neighbor bond vectors leading from site i to k , and $\boldsymbol{\sigma}$ are the spin Pauli matrices. This model respects time-reversal symmetry, and a strong topological insulator is obtained when $\delta t > 0$. We calculated the surface states on the (111) surface, and the entanglement states on a parallel cut, for the parameters $t=1.0, \lambda_{SO}=0.125, \delta t=1, t_2=0.1$. Thus, for this system, the topology of the entanglement modes is the same as that of the surface modes.

Modes protected by inversion symmetry. Our argument only showed that the entanglement spectrum has *at least as many* protected modes as the surface spectrum. In fact, inversion symmetric insulators can have phases with entanglement modes but not physical surface modes. The key point is that the imaginary cut used for defining the entanglement spectrum does not "damage" the system and its symmetry; the inversion interchanges the two sides of the cuts. Near a physical surface, there is no inversion symmetry, however.

The time-reversal symmetry of the model on the diamond lattice can be broken by applying a Zeeman field, $H_T = h \sum_i c_i^\dagger \sigma_z c_i$. Figures 1(c) and 1(d) show the surface and entanglement modes (for $h=0.9$), demonstrating a Dirac node that is protected (as we will show) by the inversion symmetry about bond centers of this model. Such a node is not present in every system [see the inset of Fig. 1(d)] but it cannot disappear without a phase transition. (The inset is the entanglement spectrum for the diamond lattice model with different parameters: the exceptional bond is *perpendicular*

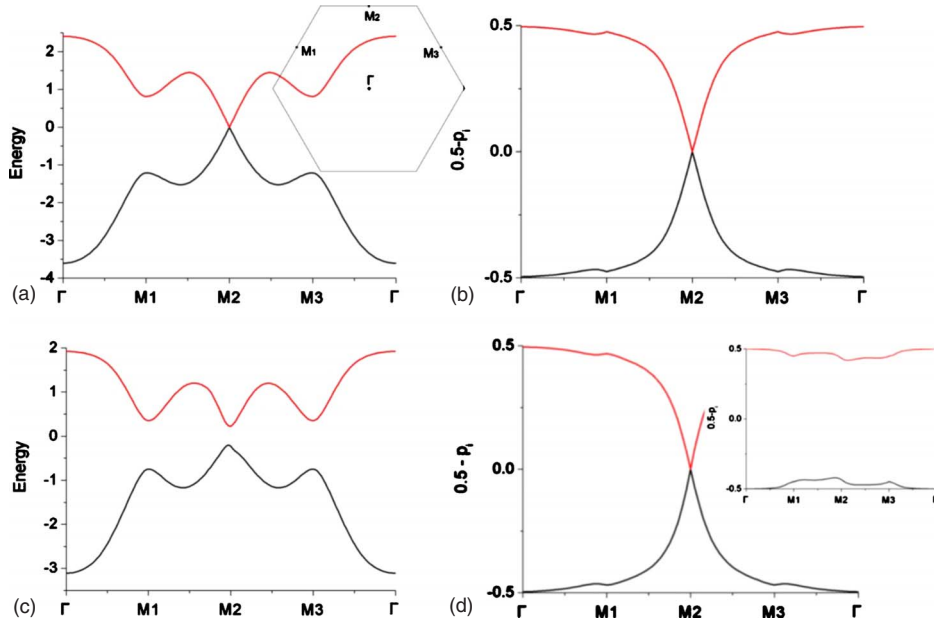


FIG. 1. (Color online) Energy modes and entanglement modes in topological insulators. [(a) and (b)] A time-reversal symmetric insulator's physical and entanglement dispersions on a cut parallel to the (1,1,1) plane (calculated along the path connecting the TRIMs M_1, M_2, M_3, Γ , as shown on the hexagonal Brillouin zone). [(c) and (d)] Inversion symmetric insulators with broken time-reversal symmetry. Note the physical surface states (c) are gapped but the Dirac node remains in the entanglement spectrum (d), at zero energy, because inversion symmetry acts as a particle-hole symmetry. Thus this phase remains distinct from one without entanglement modes (shown in the inset).

to the cutting surface and $\delta t = -.9t$. This system is a weak topological insulator with no modes along this surface.)

A mysterious property of Figs. 1(b) and 1(d) gives a clue as to how inversion is able to protect this mode: the entanglement modes are particle-hole symmetric even though (because of the second-neighbor hopping) the Hamiltonian and its surface modes are not. This suggests that the inversion symmetry \mathcal{I} of the physical Hamiltonian takes on the guise of a sort of particle-hole symmetry for entanglement. Inverting Eq. (3) gives

$$F_{i\mathbf{k}_\perp}(-x)e^{-i\mathbf{k}_\perp \cdot \mathbf{r}} = [\sqrt{1-p_i}f_{Ri}(-x) + \sqrt{p_i}f_{Li}(-x)]e^{-i\mathbf{k}_\perp \cdot \mathbf{r}}, \quad (9)$$

which has to be the same (apart from a phase) as another state of the opposite momentum $F_{i-\mathbf{k}_\perp}$ with $p_i = 1-p_i$. Since this implies $\epsilon_i = -\epsilon_i$, the operator \mathcal{I}_S (see Fig. 2) that maps between these states

$$\mathcal{I}_S f_{Li}(x) \equiv f_{Ri}(-x) \propto f_{Li}(x) \quad (10)$$

is a particle-hole symmetry.

This explains why the Dirac node in Fig. 1(b) (or any topological insulator with inversion symmetry) is at $\epsilon = 0$. The reason it remains ungapped in the magnetic field is that parities of modes cannot change discontinuously. The two modes f_a and f_b at the TRIM (see left of Fig. 3) form a Kramers doublet under time reversal; thus they have the same parity. They cannot split as the figure proposes; the two modes f_a and f_b indicated by the dots are exchanged by inversion and can thus be combined into states of opposite parities: $\frac{f_a \pm f_b}{\sqrt{2}}$.

A long-wavelength equivalent of this argument can be given for the Dirac equation $\sigma \cdot \mathbf{k} \psi = \epsilon \psi$: \mathcal{I}_S is a “CRT” symmetry (charge-conjugation times a 180° rotation times time reversal¹⁰), and acts via $\psi(x, y, t) \rightarrow \psi(-x, -y, -t)$, since $C, R,$ and T act on the spinor with $\sigma_z, \sigma_x,$ and σ_y , respectively. A mass term cannot be added without breaking this symmetry. (CPT symmetry on the other hand cannot be used to forbid a mass term, since the massive Dirac equation, like all relativistic equations, is CPT invariant.)

In general, there is a topological invariant $\Delta N(\kappa_\perp)$, defined for each TRIM as $N_+(\kappa) - N_-(\kappa)$, where $N_+(\kappa)$ and $N_-(\kappa)$ are the numbers of solutions to $\mathcal{I}_S[\phi(x)e^{i\kappa_\perp \cdot \mathbf{r}_\perp}] = \pm \phi(x)e^{i\kappa_\perp \cdot \mathbf{r}_\perp}$ among the zero entanglement-energy eigenstates. If a pair of modes moves away from zero energy, they had to start out with opposite parities, (as just shown), so $\Delta N(\kappa_\perp)$ does not change.

Inversion symmetry and the many-body spectrum. We now use the entanglement spectrum to derive some preliminary results about the effects of adding interactions. For an

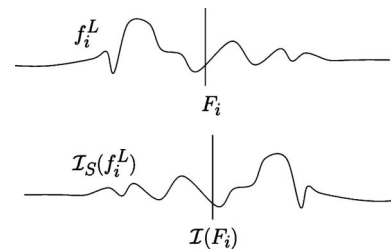


FIG. 2. The action of inversion symmetry on the entanglement modes. \mathcal{I}_S maps the left-hand half f_i^L of an F_i wave function to the inversion image $\mathcal{I}(f_i^R)$ of its other half.

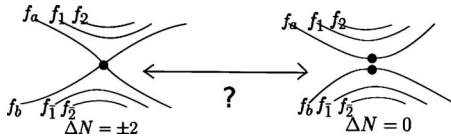


FIG. 3. Spectra that cannot evolve into one another on account of inversion symmetry. Left, a spectrum with a Dirac node; both modes at zero energy have the same parity under \mathcal{I}_S . Right, a spectrum without a Dirac node. The positive and negative energy modes interchange so they can be combined into states of opposite parity.

interacting system the many-body entanglement spectrum, Eq. (1), cannot be reduced to independent modes so we must consider the many-body version of inversion symmetry. It leads to an *antiunitary* symmetry (analogous to time-reversal symmetry, though time reversal is not present). Inversion symmetry preserves Schmidt weights but maps the states for the left half of the system to states for the right half. To remain in a fixed half of the system, combine \mathcal{I} with a second “mate” transformation \mathcal{M} , defined by $\mathcal{M}|\alpha R\rangle = |\alpha L\rangle$, and also preserving the Schmidt weights. This transformation has a consistent meaning only when extended antilinearly, $\mathcal{M}\sum_{\alpha} c_{\alpha}|\alpha R\rangle = \sum_{\alpha} c_{\alpha}^*|\alpha L\rangle$ (if extended *linearly* to superpositions of the Schmidt states, \mathcal{M} depends on the choice of phases in the Schmidt decomposition). Therefore the combination $\mathcal{M}\mathcal{I}$ is an antilinear symmetry of the Schmidt spectrum.

Now since inversion is an order-two transformation, $(\mathcal{M}\mathcal{I})^2$ has to be a pure phase for any subspace consisting of all Schmidt states of a given particle number; in particular, one can show that

$$(\mathcal{M}\mathcal{I})^2 = (-1)^{\delta} \mathbb{1} \quad (11)$$

is the same for every Schmidt state in which the fermions are split evenly between the two halves. δ is a characteristic of the insulator, and it is given in the noninteracting case by $\frac{1}{2}\sum_{\kappa_{\perp}} \Delta N_{\kappa_{\perp}}$. When δ is odd $(\mathcal{M}\mathcal{I})^2 = -\mathbb{1}$ so all states come in degenerate pairs by Kramers degeneracy.

This behavior is a consequence of the Fermi statistics of the particles. Let us check it for the topological insulator in the Zeeman field, whose Dirac doublet F_a and F_b consists of two states with the same \mathcal{I}_S parity (even, say). We will calculate $(\mathcal{M}\mathcal{I})^2$ for just the highest weight Schmidt states, which are contained in

$$|\Psi_0\rangle = \frac{1}{2}(l_a^{\dagger} + r_a^{\dagger})(l_b^{\dagger} + r_b^{\dagger})|S_L\rangle|S_R\rangle, \quad (12)$$

where $|S_R\rangle$ and $|S_L\rangle$ are the Fermi seas for the two sides. Because the states are even under \mathcal{I}_S , $\mathcal{I}l_{ab}\mathcal{I}^{\dagger} = +r_{ab}$; \mathcal{I} also exchanges the seas.

The two terms in Eq. (12) with even splits are

$$|\Psi_0\rangle = s\frac{1}{2}(|\Phi_1^L\rangle|\Phi_1^R\rangle + |\Phi_2^L\rangle|\Phi_2^R\rangle) + \dots,$$

where s is an unimportant sign and

$$|\Phi_1^L\rangle = l_a^{\dagger}|S_L\rangle, \quad |\Phi_1^R\rangle = r_b^{\dagger}|S_R\rangle,$$

$$|\Phi_2^L\rangle = -l_b^{\dagger}|S_L\rangle, \quad |\Phi_2^R\rangle = r_a^{\dagger}|S_R\rangle.$$

The crucial $-$ sign arises because of anticommutation of fermion operators, and implies the matrix representing $\mathcal{M}\mathcal{I}$ is $U_I = \begin{pmatrix} 0 & -s \\ s & 0 \end{pmatrix}$. Therefore, $(\mathcal{M}\mathcal{I})^2$, which is represented by the matrix $U_I^* U_I$, is -1 for a single node. Hence $\delta = 1$.

Even when interactions are included, Eq. (11) defines an “order parameter” δ that cannot change except at a phase transition. Interestingly, this order parameter can be determined using a *finite*-size sample of the right geometry. The parity of the ground-state wave function is $(-1)^{\delta}$ for periodic boundary conditions in the y and z directions and a finite size in x if the y and z dimensions are even. (If they are odd, one can isolate $\frac{1}{2}\Delta N_{\kappa_{\perp}}$ for a single TRIM by imposing periodic or antiperiodic boundary conditions, suggesting that at least some of the weak topological indices survive interactions.)

Furthermore, δ is related to a response function: the magnetoelectric susceptibility is given by $\frac{e^2}{2h}\delta$ (see Ref. 11).

Thus the entanglement spectrum can be used to analyze topological phases and predict their properties (here, the existence of phases with inversion symmetry) and suggests ways to generalize topological insulator properties to interacting systems (see Ref. 12).

A.M.T. would like to acknowledge Frank Pollmann and Erez Berg for working together on one-dimensional spin chains, which helped inspire some of the ideas in this Rapid Communication, and also Michael Levin for an intriguing introduction to entanglement. We thank the NSF for supporting this research with Grant No. NSF-DMR-0645691.

¹M. Hasan and C. Kane, *Rev. Mod. Phys.* **82**, 3045 (2010); X.-L. Qi and S.-C. Zhang, *Phys. Today* **63**(1), 33 (2010); J. Moore, *Nat. Phys.* **5**, 378 (2009).

²H. Li and F. D. M. Haldane, *Phys. Rev. Lett.* **101**, 010504 (2008).

³L. Fidkowski, *Phys. Rev. Lett.* **104**, 130502 (2010).

⁴I. D. Rodríguez and G. Sierra, *Phys. Rev. B* **80**, 153303 (2009).

⁵F. D. M. Haldane, Proceedings of the APS March Meeting, 2009 (unpublished).

⁶N. Bray-Ali, L. Ding, and S. Haas, *Phys. Rev. B* **80**, 180504(R) (2009).

⁷I. Peschel, *J. Phys. A* **36**, L205 (2003).

⁸A. Botero and B. Reznik, *Phys. Lett. A* **331**, 39 (2004); I. Klich, *J. Phys. A* **39**, L85 (2006).

⁹L. Fu, C. L. Kane, and E. J. Mele, *Phys. Rev. Lett.* **98**, 106803 (2007).

¹⁰This combination acts unitarily on single-body states and transforms \mathbf{k}_{\perp} , ϵ^{ℓ} in the same way as \mathcal{I}_S .

¹¹A. M. Turner, Y. Zhang, R. S. K. Mong, and A. Vishwanath, [arXiv:1010.4335](https://arxiv.org/abs/1010.4335) (unpublished); T. L. Hughes, E. Prodan, and B. A. Bernevig, [arXiv:1010.4508](https://arxiv.org/abs/1010.4508) (unpublished).

¹²L. Fidkowski and A. Kitaev, [arXiv:1008.4138](https://arxiv.org/abs/1008.4138) (unpublished); A. M. Turner, F. Pollmann, and E. Berg, [arXiv:1008.4346](https://arxiv.org/abs/1008.4346) (unpublished).